Journal Pre-proofs

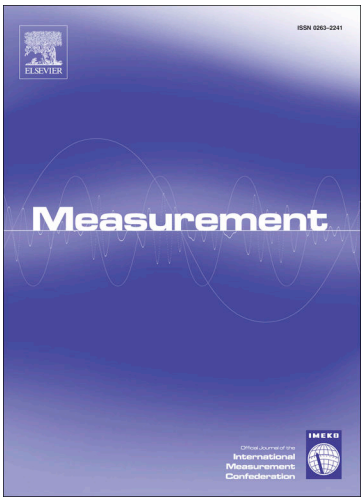

Application of Ultrasound Techniques in Solid-Liquid Fluidized Bed

Fria Hossein, Massimiliano Materazzi, Matteo Errigo, Panagiota Angeli, Paola Lettieri

PII: S0263-2241(22)00285-8
DOI: https://doi.org/10.1016/j.measurement.2022.111017
Reference: MEASUR 111017

To appear in: *Measurement*

Received Date: 10 January 2022
Revised Date: 1 March 2022
Accepted Date: 7 March 2022

Please cite this article as: F. Hossein, M. Materazzi, M. Errigo, P. Angeli, P. Lettieri, Application of Ultrasound Techniques in Solid-Liquid Fluidized Bed, *Measurement* (2022), doi: https://doi.org/10.1016/j.measurement.2022.111017

Application of Ultrasound Techniques in Solid-Liquid Fluidized Bed

Fria Hossein*, Massimiliano Materazzi, Matteo Errigo, Panagiota Angeli, Paola Lettieri

Department of Chemical Engineering, University College London, London, WC1E 7JE, United Kingdom.

***f.hossein@ucl.ac.uk**

Abstract

This paper describes an application of ultrasound techniques to solid-liquid fluidized beds. The ultrasonic methods, experimental setups, and the signal processing for obtaining velocity profiles, particle size distribution, and solids volume fraction are discussed. The techniques are based on the measurement of the ultrasound attenuation coefficient, sound speed, and frequency shift of the propagated sound wave. The ultrasound propagation speed in solid-liquid fluidized bed was measured to be between 1504 m/s to 1565 m/s for glass particles with volume fractions spanning from 27% to 70% in water. The solid velocity profiles were measured for liquid superficial velocities varying from 0.84 cm/s to 4.24 cm/s. The particle size distributions were measured for four different sizes of glass particles ranging from 500 μm to 1250 μm at a solid volume fraction of 35%. This paper also reports the importance of the techniques as a diagnostic tool to investigate the particles segregation behaviour in solid-liquid fluidized beds at different fluidization conditions. The results indicated that ultrasound techniques are a powerful tool that can characterise in real-time highly concentrated solid-liquid systems.

Key Words:

Fluidization, Velocity Profile, Voidage, Attenuation, Ultrasound, Particle Sizing, Algorithm, Inversion, segregation.

1. Introduction

Fluidized-bed reactors have very broad and extensive industrial applications, mostly in the chemical, biomedical and nuclear power generation fields (Cocco et al., (2014)). To understand and be able to predict the behaviour of these complex systems it is of paramount importance to measure different parameters, such as fluid and particle velocity profiles, particle size distribution and voidage (fluid volume fraction) during operation. Currently no single technique available enables the measurement of all these parameters. The aim of this paper is to introduce ultrasound-based techniques, which can measure these quantities in real time in liquid-solid fluidized beds. Particle size characterization in fluidized bed systems is of great importance to their application in energy generation, materials preparation, and pharmaceutical industries. Measuring the particle size distribution (PSD) is significant when it changes over time, due to agglomeration or particle breakage in thermochemical systems (Lin et al., (2011), Iannello et al., (2020)), polymerisation or attrition (Yates and Lettieri, (2016)), and in biological wastewater treatment (Garbowski et al., (2019)). Acoustic emission technique could be used to the study of fluid-particle flows; recently acoustic emission waveform was used to obtain detailed structural characteristics of coal rock masses at different loading stages (Li et al., (2021)-b, Li et al., (2021)-a). Ultrasound technique can be used to observe particle segregation patterns and can be useful to understand and optimize the hydraulics of a fluidized-bed reactor. On the other hand, solid particle velocity and voidage profiles provide useful information on the fluidization quality. Being able to non-invasively determine these quantities while the fluidized bed is operating would represent a great diagnostic tool, useful to improve the operation of industrial systems.

Several measurement techniques have been developed to characterize dispersed phases in opaque fluidized bed systems, such as impedance and optical fibre probes (Taofeeq and Al-Dahhan, (2018), Tortora et al., (2008)). Currently, axial voidage profiles can be obtained from local pressure measurements (Saadevandi and Turton, (2004)), electrical capacitance (Sines et al., (2019)) and optical probes (Liu et al., (2003)). The physical principles behind the last two techniques are, respectively, the differences in the electrical properties between various phases in the case of impedance probes, (Spinelli et al., (2019)) and in the light transmission properties for optical fibre probes (Muñoz-Cobo et al., (2017)). However, the optical probe techniques are invasive, affecting the fluid dynamics of the bed. Techniques based on electromagnetic radiation attenuation for obtaining voidage distribution, such as γ-ray or x-ray imaging (Materazzi et al., (2017)) rely on the differences in density of different materials. Their applications to liquid-solid fluidized beds, where this difference is fairly small, are therefore limited (Panariello et al., (2017)). Current techniques to measure the solid particle velocity field are particle image

velocimetry (Laverman et al., (2008)), optical fibre Doppler frequency shift (Evseev, (2016)), positron emission particle tracking (PEPT) (Langford et al., (2016)) and computer-automated radioactive particle tracking (CARPT) (Mosorov, (2013)). In particle image velocimetry tracer particles must be inserted with refractive index that matches that of the liquid and of the other particles, significantly limiting the materials that can be used. On the other hand, the optical fibre Doppler frequency shift technique is invasive, while the last two tracking methods are not appropriate for online diagnostics, as they follow one particle at a time and need further statistical post-processing to provide the particles velocity field. Finally, particle size distribution and segregation patterns in a fluidised-bed reactor can be obtained by sampling the particles at different heights (Chen and Keairns, (1975)) or at the top of the bed (Di Renzo et al., (2020)) while the reactor is operating. Alternative techniques include stopping the flow to freeze the bed and then measuring the pressure drop for small flow rates along the column (Lam Cheun U, (2010)) or applying image analysis to a pseudo-2D fluidized bed system (Obuseh et al., (2012)). From these techniques, sampling particles and using local pressure drop are not suited to online measurements. The local pressure measurements can only determine an average particle size, rather than a distribution. The last approach is only applicable to 2D reactors with transparent walls, which are not common in industrial applications.

Ultrasound techniques offer a valid alternative to the above approaches as they have many desirable characteristics; they are non-intrusive, have fast response and low cost, allowing for cheap, online measurements of non-transparent test sections(Hossein, (2019), Hossein and Wang, (2019)). (Vatanakul et al., (2005)) used ultrasound attenuation and speed to measure the phase hold up in air-water-solid circulating fluidized bed. In this study we develop the ultrasound techniques to characterise particle velocity profile and particle size distribution (PSD) beyond the phase hold up, in liquid-solid fluidized beds. The ultrasound techniques used here are based on the measurements of the sound attenuation and speed to characterise the voidage of the bed, of the Doppler effect to obtain the solids velocity profiles, and of the attenuation coefficient at different sound excitation frequencies to characterise the particle size distribution. The Doppler effect manifests itself as a change in the frequency of the sound wave when it impacts objects moving at a different velocity with respect to the sound source and is widely used in medicine (Chun et al., (2011), Sigel, (1998)); in multiphase flows it has been used to obtain velocity profiles of solid particles in dispersed liquid-solid flows (Meribout et al., (2020), Tomonori et al., (2013), Takeda. Y., (2013)) and of bubbles in bubbly flows (Aritomi et al., (2000)). Ultrasound has been used to analyse the particle size distribution in sample cells for solid concentrations up to 10% (Nan et al., (2019), Patricia and Derek, (2000)) and a range of particle sizes, up to 30 μm (Thao et al., (2016)).

In this work we develop the ultrasound techniques and signal processing to characterize the velocity profiles and size distribution of particles in addition to volume fraction in highly concentrated fluidized beds, with up to 35% particles volume fraction, for the first time. Previous works have obtained phase hold up in fluidized beds (Vatanakul et al., 2005) or only studied the variation of the sound speed and attenuation in suspensions of particles in sample cells or small vessels (Dion and Burns, (2011), Huang et al., (2013), Hossein and Wang, (2020)). We also propose a new approach to measure the velocity profile of the solids, based on the use of two transducers. The conventional use of a single transducer for velocity profile measurements leads to a large error because both the transmitted and the reflected signals travel through the same path in the mixture. Furthermore, when the probe switches from the transmitting to the receiving mode, there is some loss of the signal. The use of multiple sensors overcomes these issues. In what follows, the materials used, and the methodologies developed are discussed in Section 2. Section 3 details the results and discussions, and Section 4 summarises the conclusions.

2. Materials and Methods

The experiments were conducted in a vertical fluidized bed made of a borosilicate glass tube, which is 0.4 cm thick, 80 cm high and has an inner diameter of 5 cm (see Figure 1). The top of the tube has a stainless-steel dutch weave mesh to prevent suspended particles from escaping. Water (tap water with density of 1000 kg/m^3) is pumped into the bed through a distributor, which is made of another stainless-steel dutch weave mesh with a hole size of 500 μm. The role of the distributor is to evenly distribute the water across the bottom of the bed and avoid the backflow of particles. The flowrate is controlled via two manual rotameters. It is assumed that the temperature is constant and equal to room temperature.

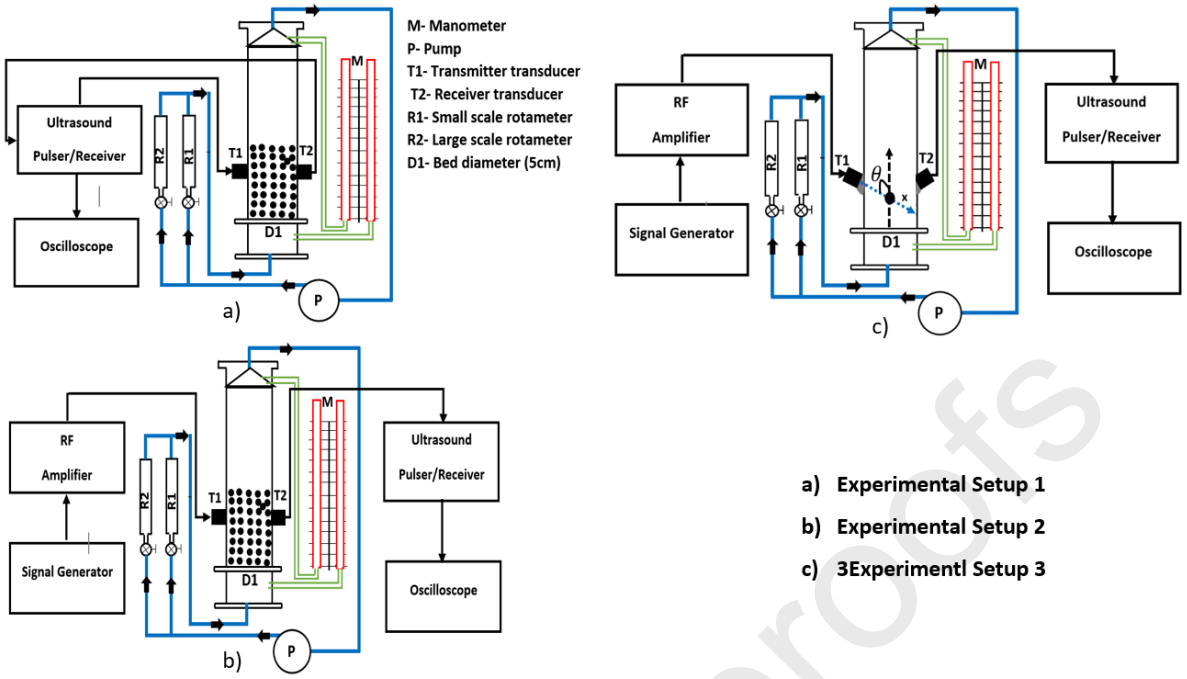

Figure 1: Diagram of the liquid-solid fluidized bed with a sketch of the a) ultrasound attenuation and speed measurement setup, b) ultrasound spectroscopy measurements, c) UVP measurement.

The bed is initially made of glass beads with a density of 2500 kg/m^3. Beads of different diameters (as provided by the manufacturer) were used, as shown in Table 1. Sample 4 in Table 1 was obtained by mixing equal masses of samples 2 and 3. The minimum fluidization velocities, U_{mf}, for each size, at which the bed starts to expand, are also shown. They were obtained experimentally from fluidization curves of pressure drop across the bed against liquid superficial velocity. The pressure drop increases with increasing liquid velocity until the point of fluidization, where the liquid velocity is large enough for the drag force on the particles to balance their weight; beyond this point, the pressure drop is constant. The minimum fluidization velocity can be obtained from the intersection of the two lines fitting the experimental data below and above the fluidization point. These minimum fluidization velocities are a function of the particle size and density, as well as of the density and viscosity of the liquid.

Moreover, the average minimum fluidization velocity of sample 4 was obtained both with a correlation for binary mixtures (Owoyemi, (2007)) and experimentally by the means of the pressure drop curves. The first technique returned a value of 0.78 cm/s, while the second one led to a minimum fluidization velocity of 0.96 cm/s. The two results are consistent with each other, and the discrepancy is possibly due to a combination of experimental error and the fact that the correlation for binary mixtures does not take into account certain properties, such as the

width of the particle size distribution. Both of them, however, are significantly lower than the larger particle minimum fluidization velocity, as expected (Yang, (2003)). The experimentally derived minimum fluidization velocity U_{mf} will be used here.

Table 1: Prepared samples for ultrasound spectroscopy test

Sample	Particle Diameter Range (Manufacture) [µm]	Weight [gram]	Minimum Fluidization superficial velocity U_{mf} [cm/s]
1	500-600	443	0.28
2	750-1000	443	0.75
3	1000-1250	443	1.19
4	750-1250	443	0.96

The particle size distributions of each of the three unmixed samples, to be used as a reference, were obtained from images with a border recognition code based on the Matlab function *imfindcircles*. The results are shown in Figure 2.

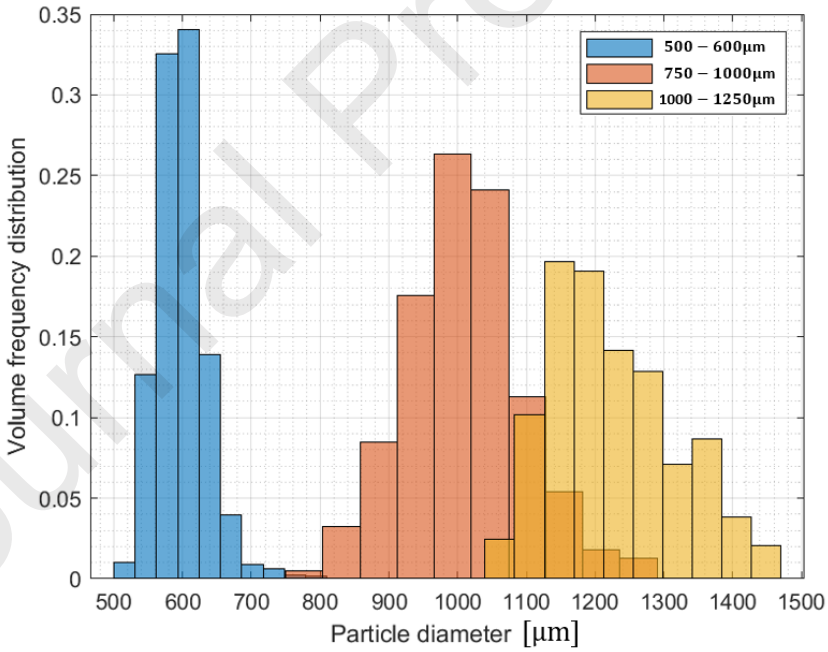

Figure 2. Particle size distributions of the three samples.

When the liquid superficial velocity is larger than the minimum fluidization velocity U_{mf}, the bed starts expanding and the solid-liquid mixture starts behaving like a single phase fluid. Since the fluidizing agent is a liquid, there will be no formation of bubbles, while as the flow rate increases, the fluidized bed will continue to expand (Ghatage et al., (2014)). The values of the

liquid flow rate and of the corresponding bed height are measured respectively via the rotameters and a tape measure on the fluidized-bed wall. The bed height h_b allows for the computation of the bed voidage, ε. Table 2 shows the voidage values for 0.55 kg of sample 1 particles. Knowing the mass and the density of the particles, respectively m_p and ρ_p, as well as the inner diameter, D_b, of the fluidized bed, the voidage is calculated according to the following Equation:

$$\varepsilon = 1 - \frac{m_p}{\rho_p \cdot \pi \cdot \frac{{D_b}^2}{4} \cdot h_b} \quad \textbf{(1)}$$

Table 2. Experimental conditions for ultrasound attenuation measurements in the liquid-solid fluidized bed (mass of the sample 1 particles: 0.55 kg).

Liquid Flow Rate $[L/min]$	U/U_{mf} [-]	Bed Height $[cm]$	Bed Expansion $[cm]$	Average (calculated) voidage $[-]$
0	0	18.4	0	0.391
0.5	1.5	19.2	0.8	0.416
1	3	22.9	4.5	0.511
1.5	4.5	25.5	7.1	0.561
2	6	28.4	10	0.605
2.5	7.6	31.9	13.5	0.649
3	9	36.9	18.5	0.696
3.5	10.6	41.4	23	0.729

For the measurements of the various bed properties using ultrasound techniques, different settings were used, as described below.

Experimental setup 1: Ultrasound propagation speed and attenuation for voidage measurements

To obtain the fluidized bed voidage, the ultrasound propagation speed or the attenuation coefficient need to be measured. A diagram of the position of the transducers transmitting (T_1) and receiving (T_2) the ultrasound signal is shown in Figure 1a. Transducers used in our experiments were manufactured by Sonatest, (Sonatest RTD2250 ¼'' in diameter, Resonance frequency 5 MHz, Delay Line, MICRODOT). To receive the best possible signal, the alignment of the transducers is pivotal. The ultrasound excitation signal is generated by an ultrasonic pulser/receiver (JSR Imagining Pulser/Receiver DPR 300) and is sent through the liquid-solid fluidized bed via the transducer T_1. The propagated signal is captured by the second transducer

T_2 and is collected via the same ultrasound pulser/receiver. The signal received is attenuated with respect to the transmitted one, mostly due to the interaction of the ultrasound with the liquid-solid interfaces, and, for this reason, the received signal is amplified by up to 50 dB. The signal is then displayed on an oscilloscope screen (Keysight-DSOX3014T, 4-channel, 100 MHz). The digitized signal is downloaded from the oscilloscope to a computer for further signal processing.

To measure the ultrasound attenuation in the glass beads-water mixture, a reference for the propagated signal is required. As reference, the signal transmitted through the liquid phase (tap water) only is taken. The received reference signal and its Fast Fourier Transform (FFT) are shown in Figure 3.

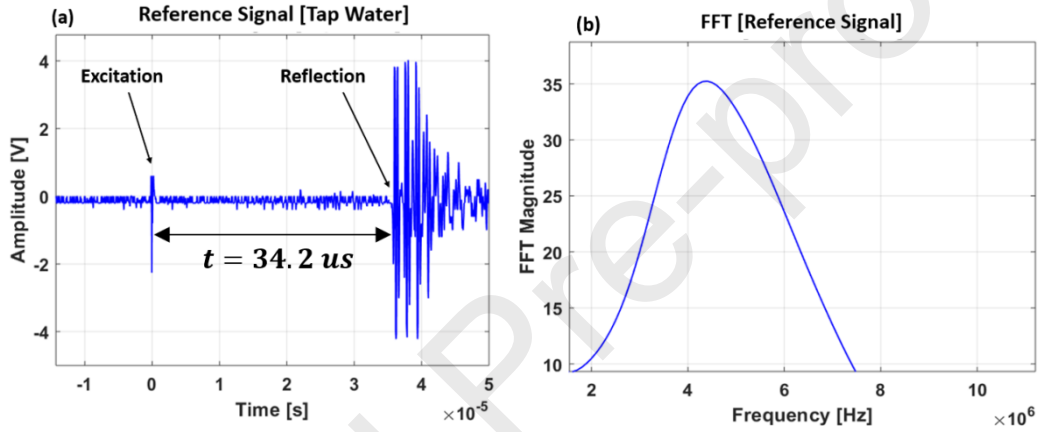

Figure 3: (a) The reference signal for ultrasound attenuation with a frequency of 5 MHz (amplified by 30 dB), and (b) its FFT magnitude.

The maximum amplitude of the received reference signal, A_o, is found equal to 35.24 V, using an amplification of 30 dB $\left(\text{Gain} = 20\log\left(\frac{V_{out}}{V_{in}}\right)\text{dB}\right)$, meaning that the signal before the amplification is equal to 1.11 V.

To calculate the ultrasound speed in tap water inside the tube with an inner diameter of 5 cm, the following Equation can be used:

$$C = \frac{D_b}{t} \quad \textbf{(2)}$$

where t is the arrival time of the propagated sound wave, D_b is the tube diameter, and C is the ultrasound speed in the liquid (water) phase. The arrival time of the signal is equal to t = 34.2

μs, as can be seen in Figure 3a. The time required for the signal to travel through the 0.4 cm thick borosilicate glass wall was measured previously and found equal to 0.8 μs. The speed of sound in tap water was then found equal to $1462\ \mathrm{m/s}$. The signal processing methodology to calculate the bed voidage from both sound speed and attenuation measurements is discussed in section 3.

Experimental setup 2: Attenuation spectroscopy for particle size distribution measurements

A schematic representation of the experimental setup for the ultrasound attenuation spectroscopy measurements is shown in Figure 1b. The main difference with respect to the experimental setup 1 is the use of a signal generator and radio frequency (RF) amplifier for a fine control over the ultrasound signal characteristics. For each experiment, the sample particles were placed into the bed. In order to have a fully expanded bed, the liquid superficial velocity was set to $2.1\ \mathrm{cm/s}$, which is three times above the minimum fluidization velocity of all particle sizes considered. The resulting values are reported in Table 3, together with the bed voidage for each sample at the liquid superficial velocity of 2.1 cm/s, calculated according to Equation 1.

Table 3. Minimum Fluidization velocity U_{mf} and bed voidage at the chosen liquid superficial velocity of 2.1 cm/s for each sample.

Sample	Particle Size Range (Manufacture) [μm]	Minimum Fluidization velocity U_{mf} [cm/s]	Bed voidage at 2.1 cm/s [-]
1	500-600	0.28	0.70
2	750-1000	0.75	0.56
3	1000-1250	1.19	0.47
4	750-1250	0.65	0.58

For the spectroscopy measurements, signals are generated (with a frequency ranging between 2 MHz to 8 MHz) by the waveform signal generator and amplified by 30 dB by the RF amplifier. The amplified signal is sent through the fluidized bed via transducer T_1. The propagated signal is then captured by transducer T_2 and collected by the ultrasound pulser/receiver. The signal received is attenuated with respect to the transmitted one, mostly due to the interaction of ultrasound with the liquid-solid interfaces, and, for this reason, it is amplified by up to 70 dB. The signal is then displayed on the oscilloscope screen and downloaded to a computer for further signal processing.

To measure the attenuation coefficient in the bed at different excitation signal frequencies, a reference signal is required, and this is obtained by sending the signal through the liquid phase (water) only in the fluidized bed. An example of the reference frequency spectrum at different excitation frequencies is shown in Figure 4. The received signal spectrum is found through processing the raw received signal via FFT.

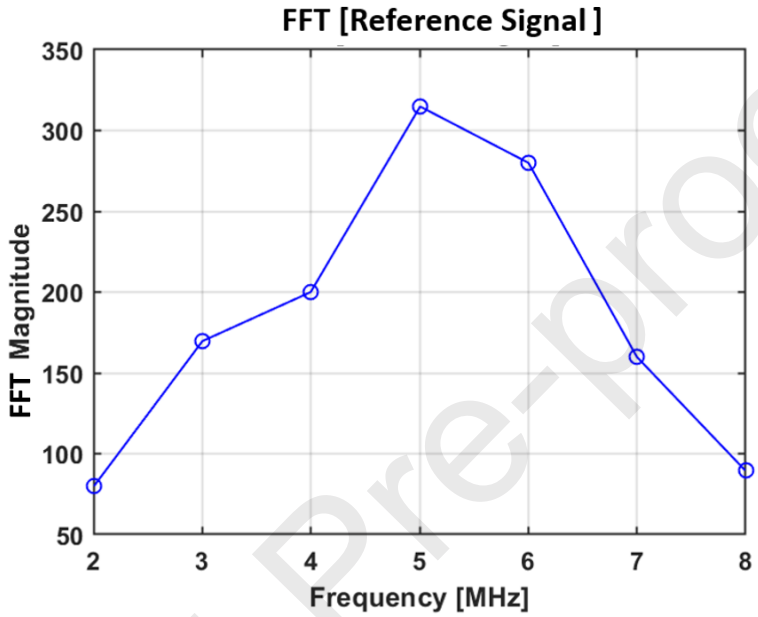

Figure 4: The maximum value of the FFT (Fast Furious Transform) of the reference signal spectrum for different excitation signal frequencies (x-axis).

Experimental setup 3: Doppler effect for velocity profile measurements

Figure 1c illustrates the ultrasonic velocity profile (UVP) measurement system for obtaining the solid particles velocity profile. The setup is similar to setup 2, with the use of a signal generator and an RF amplifier for a fine control over the ultrasound signal characteristics. In contrast to the previous two set ups, the transducers are placed at an inclination angle of 45°, on opposite sides of the fluidized bed wall, to ensure the capture of the velocity component in the direction of the measurement line. Some ultrasound gel was applied to eliminate air between the transducers and the fluidized bed wall. For these experiments, the particle sample 1 was used and the liquid superficial velocity, U, was initially set to 0.84 cm/s, which is three times above the minimum fluidization velocity, and increased progressively by 0.84 cm/s up to 4.24 cm/s.

An ultrasound signal with a frequency of 5 MHz and 4 cycles is emitted from the signal generator and amplified before it is transferred to the emitting transducer T_1. The signal is scattered by the moving particles along the measurement line x (see Figure 1c), and the scattered signal is received by transducer T_2. The received signal is amplified by up to 46 dB by the pulser/receiver, is displayed on the oscilloscope screen and downloaded to a computer for further signal processing. The received signal contains both the initial and the shifted frequencies. The inclination angle of the transducers $\theta = 45°$ and the angle between the flow direction and the measurement line x (see Figure 1c) are assumed to be the same, neglecting refraction, because the difference between the density of the ultrasound gel and of the tap water is small and it can be ignored (Hossein et al., (2021)).

It is possible to measure all three properties with the same setup. However, for the particle size distribution the signal must be emitted with at least three or more different frequencies, while for the measurement of the velocity profile, the transducers must be mounted with an inclination angle. The hardware in Set up 2 (which is the same as in Set up 3) could be used for all measurements: using a single frequency for the void fraction measurements or inclining the transducers for the velocity profile measurements.

3. Results and Discussion

3.1 Voidage profile measurements

To measure the voidage profile in the liquid-solid fluidized bed, the experimental setup 1 is used. For the voidage measurements, 0.55 kg of particle sample 1 were placed into the bed. The signal is sent through the liquid-solid mixture and the liquid superficial velocity is varied, while the received signal is amplified by up to 50 dB. The transducers are mounted on the bed wall at a height of 11 cm above the distributor plate. Two different techniques have been employed to measure the voidage in the bed, namely the attenuation coefficient and the ultrasound speed in the bed. The liquid superficial velocity was varied between $0.42\ \mathrm{cm/s}$ and $3.0\ \mathrm{cm/s}$, with increments of $0.42\ \mathrm{cm/s}$, in order to study the fully expanded behaviour of the bed.

Attenuation measurements: The bed height was measured at different liquid flowrates. The ultrasound attenuation coefficient (α), as the signal travels through a medium over a length D_b (the inner diameter of the tube in this case, which is $5\ cm$) can be calculated by:

$$A_i = A_o e^{-\alpha D_b} \quad \textbf{(3)}$$

where, A_i is the attenuated amplitude and A_o is the reference amplitude (see Figure 3b) of the sound wave.

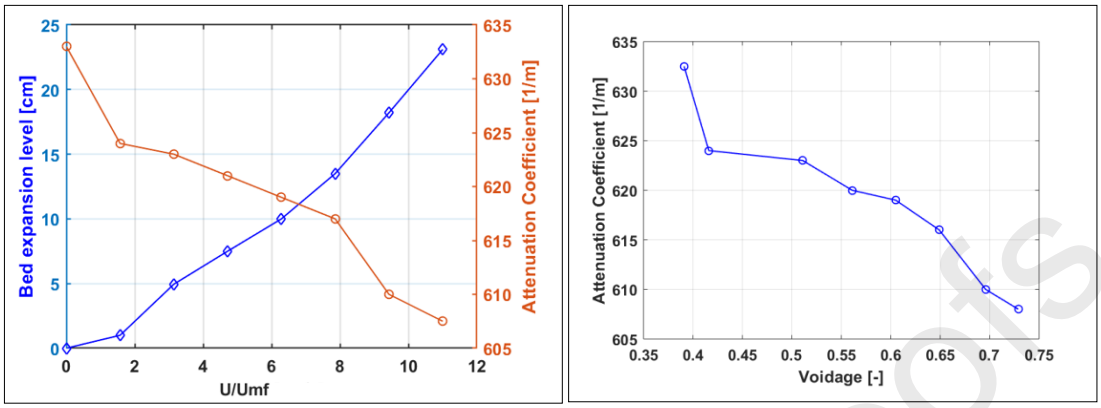

(a) (b)

Figure 5: (a) Ultrasound attenuation coefficient (orange colour) and bed expansion (blue colour) vs liquid superficial velocity (U)/minimum fluidization superficial velocity (U_{mf}) in the liquid-solid fluidized bed with sample 1 particles. (b) Ultrasound attenuation coefficient vs bed voidage.

In Figure 5a the attenuation coefficient and bed expansion height are plotted against the ratio of the liquid superficial velocity (U) over the minimum fluidization superficial velocity (U_{mf}). From the bed height, the bed voidage can be calculated using Equation 1 (see also Table 2). As can be seen in Figure 5b the attenuation coefficient reduces as the bed voidage increases, and this agrees with previous studies (Macchi et al., (2001)).

At rest, the packed bed height is equal to 18.4 cm; with the liquid superficial velocity increased to $2.5\ \mathrm{cm/s}$, the bed height expands to $36.9\ \mathrm{cm}$ (see Figure 5a). At these conditions, the ultrasound attenuation coefficient was measured at various bed levels, and it was found to vary between $607\ \mathrm{m}^{-1}$ to $609\ \mathrm{m}^{-1}$ as can be seen in Figure 6. The results indicate that the bed is expanding more or less uniformly. The error bars in Figure 6 are determined by dividing the standard deviation, σ, of the measurements by the square root of the number of measurements, N, in our case $\mathrm{N} = 5$.

$$\mathrm{error} = \frac{\sigma}{\sqrt{\mathrm{N}}} \tag{4}$$

The potential measurement error could be due to a transducer misalignment, which would affect the strength of the measured transmitted signal.

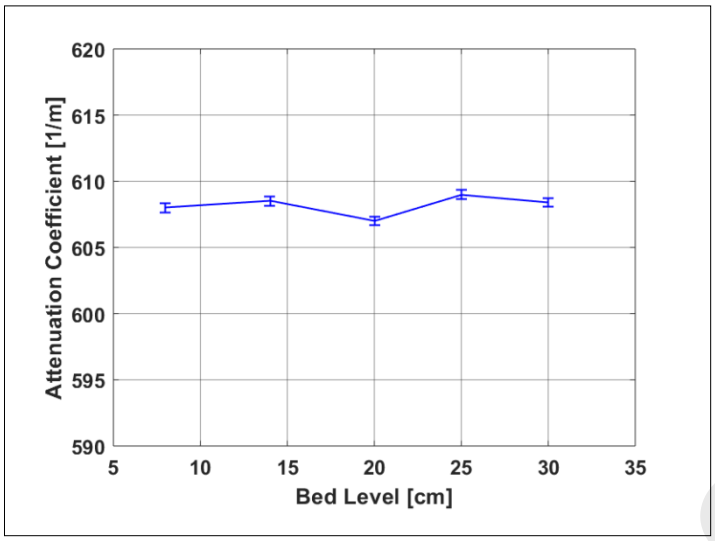

Figure 6: Ultrasound attenuation coefficient measured at different bed heights for a fixed liquid superficial velocity (2.5 cm/s).

Sound speed measurements: In this work the average bed voidage can also be obtained by measuring the ultrasound speed in the mixture. The ultrasound propagation speed in solid-liquid mixtures for different concentrations has been reported by (Atkinson and Kyto¨maa, (1993)). The ultrasound speed through the bed was calculated using Equation 2. The variation of the ultrasound speed with the bed voidage is presented in Figure. 7, based on the average of three experiments, giving a standard deviation of less than 0.21%. It was found that, by increasing the liquid superficial velocity, and therefore increasing the bed voidage, the arrival time of the signal was increased. This is in accordance with the expectation that the larger the voidage is, the slower the ultrasound signal will travel, since the ultrasound speed in water is smaller than the ultrasound speed in glass. The phenomenological model by (Uric, (1947)) can be used to theoretically calculate the sound speed in a mixture, C_{mix}, when both the effective density ρ_{eff} and the effective compressibility β_{eff} of the mixture are known.

$$C_{mix} = \frac{1}{\sqrt{\rho_{eff}\beta_{eff}}} \quad \textbf{(5)}$$

$$\rho_{eff} = \rho_s\varphi + \rho_f(1-\emptyset) \quad \textbf{(6)}$$

$$\beta_{eff} = \beta_s\varphi + \beta_f(1-\emptyset) \quad \textbf{(7)}$$

where, ρ_f and ρ_s are the densities of the fluid (water) and of the glass particles, respectively, β_f and β_s are the compressibility of the fluid (water) and of the glass particles, respectively, and $\emptyset$

is the volume fraction of the particles. Urick's model is more appropriate when the dispersed material has an acoustic impedance close enough to that of the continuous phase; the model, however, does not consider the effect of the fluid viscosity and of the particle size. Harker and Temple, (1988) improved Urick's expression by including the effect of fluid viscosity and particle size as follows:

$$\rho_{eff} = \varphi\emptyset + (1-\emptyset)\rho_f - 2(\rho_s-\rho_f)^2\emptyset(1-\emptyset)Q/(Q^2+\mathcal{B}^2) \quad (8)$$

$$Q = 2(\rho_s-\rho_f)(1-\emptyset) + \frac{9}{2}\left(\frac{\delta}{R}\right)\rho_f + 3\rho_f \quad (9)$$

where, R is the particle radius, $\delta=\sqrt{2\eta/\omega\rho_f}$, η is the water viscosity, ω is the angular frequency of the emitted ultrasound signal, and the term $\mathcal{B}$ is given by (Harker and Temple, (1988)):

$$\mathcal{B} = \frac{9}{2}\rho_f\left\{\left(\frac{\delta}{R}\right) + \left(\frac{\delta}{R}\right)^2\right\} \quad (10)$$

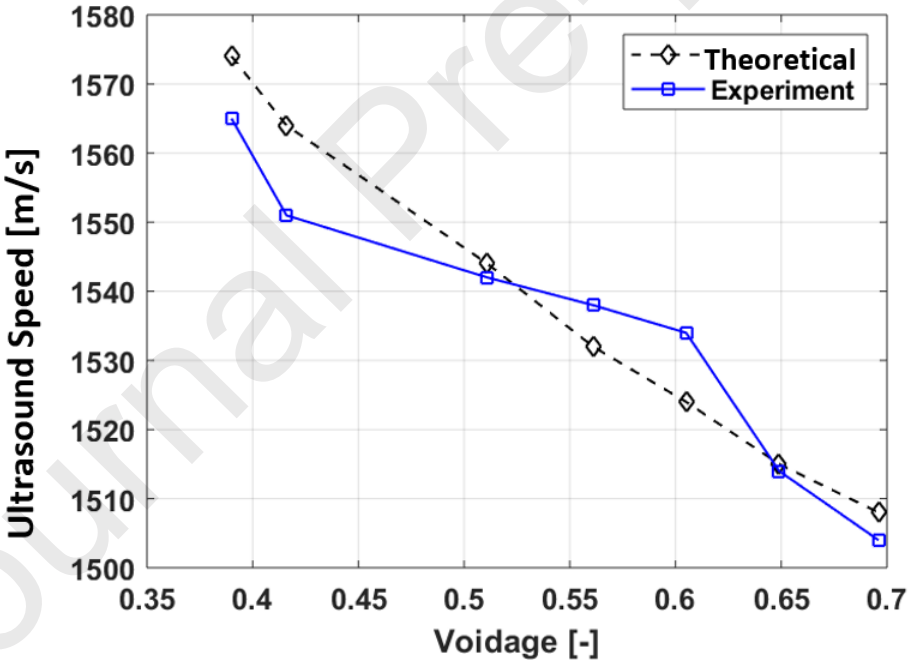

Figure 7: Ultrasound speed in liquid-solid mixture as predicted from the expression introduced by (Harker and Temple, (1988)) (black line) and measured ultrasound speed in liquid-solid fluidized bed as a function of the bed voidage (blue line).

Equation 8 and Equation 7 are used for the predictions of ultrasound speed in Equation 5, and the predicted ultrasound speed is compared against the measured one in Figure 7 for different values of bed voidage. The differences between the measured and predicted results may be attributed to the effect of the liquid velocity to the ultrasound speed, which is not accounted for in Equation 8.

Figure 5(b) or Figure 7 can be used to obtain the bed voidage at different heights for the systems described above. This information can be useful when analysing nontransparent systems (e.g., metal vessels) to study the bed expansion and voidage at different fluid flowrates.

3.2 Particle Size Distribution (PSD) measurements

The ultrasound attenuation spectra that are acquired in the excitation frequency range of 2-8 MHz are used to determine the particle size distribution using the experimental setup 2. To enable this, the following are required: a mathematical model to interpret the ultrasound spectrum (Su et al., (2008)), the measurement of the ultrasound attenuation coefficient over a range of frequencies, and the retrieval of the PSD. The physical mechanisms occurring in the interaction between particles and ultrasonic waves include scattering losses, viscous inertial dissipation (particles will oscillate due to the density difference between the particle and the liquid and this converts part of their energy into heat) and absorption, which is not related to the particle size. The attenuation coefficients of the different samples of glass beads with a solid volume fraction of 35% at liquid superficial velocity equal to $2.1\ \mathrm{cm/s}$ are calculated from Equation 3 and presented in Figure 8 for a range of ultrasound transmitting frequencies.

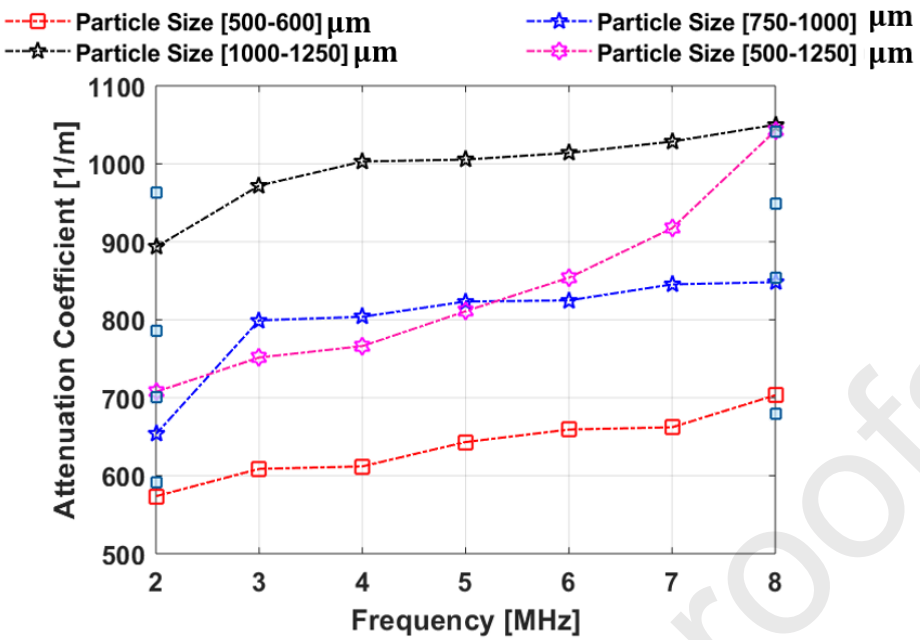

Figure 8: Ultrasound attenuation coefficient spectra of glass beads (transmitting signal frequency x-axis, attenuation coefficient y-axis).

The attenuation coefficient measurements versus the frequency of the emitted waves are presented in Figure 8. The attenuation coefficient measurements were repeated three times, and based on the average of three experiments, giving a standard deviation of less than 0.23%. An inversion algorithm is required to estimate the particle size distribution from the experimental measurements of the attenuation coefficient. The calculation of particle size distribution is not only related to the frequency dependence of the ultrasound attenuation spectra but also depends on the theoretical model and inversion algorithm. The best model should provide minimum error between the calculated and measured ultrasound attenuation spectra. The optimum regularization technique is an independent model, which is improved by optimizing the regularization factors combined with mathematic operations such as Generalized Cross Validation, to solve the ill-conditioned equations and yield a higher stability of solution (Jia et al., 2019). We adapted the optimum regularization technique model here, because of its simplicity, and accuracy. It provides less error between the measured and calculated attenuation coefficient spectra compared to Broyden-Fletcher-Goldfard-Shanno algorithm (Head and Zerner, (1985)), Levenberg-Marquard algorithm (Moré, (1978)), and Genetic algorithm (Yang et al., (2016)). and thus, results to better measurement of particle size distribution.

One model which links the attenuation coefficient to the frequency is the ECAH (Epstein, Carhart, Allegra and Hawley) model, which considers the ultrasound attenuation coefficient as the sum of the scattering effects from each particle (Allegra and Hawley, (1972)). In the ECAH model the attenuation coefficient, α, is given by:

$$\alpha = \alpha(f,\emptyset,R,P) \tag{11}$$

where, f is the ultrasound emission frequency, $\emptyset$ is the particle volume fraction, R is the particle radius while the physical vector P contains all the physical properties. The ultrasound attenuation in the fluid-particle system is taken as the sum of the scattering effects from each particle size, and is expressed as (Su et al., (2008)):

$$\alpha = \frac{3\emptyset}{2k_c^2}\sum_{j=1}^{N}\frac{q_j}{R^3}\sum_{n=0}^{\infty}(2n+1)\mathrm{Re}[A_n(R_j,\omega)] \tag{12}$$

where, $j = 1$ to N, $k_c = \frac{2\pi}{\omega}$, is the wavenumber of the emitted wave, ω is the angular frequency, q_j is the volume fraction of particles with size in the range of $[R_j + R_{i+1}]$, A_n is the scattering coefficient, and can be calculated by different approaches available in the literature (Hay and Mercer, (1985)), (Temkin, (2000)). A_n is a function of k_cR. The integer $n = 0,1,2,3...$ corresponds to the nth partial wave. Su et al., (2007), reported the variation of the scattering coefficient A_n versus integer $0 \le n \le 7$, for a particle size distribution and showed that the scattering coefficient decays dramatically for small particles, but is constant for larger particles.

Equation 12 can be used to calculate the ultrasound attenuation coefficient theoretically, and it reveals the theoretical basis for particle size measurement by using the measured attenuation coefficient spectrum. The matrix form of Equation 12 is expressed by (Nan et al., (2019)) as:

$$\underbrace{\alpha(\omega)}_{G_i} = \underbrace{\frac{3\emptyset}{2}\int\frac{1}{R^3k_c^2}\sum_{n=0}^{\infty}(2n+1)A_n\,dr}_{A_{ij}}\underbrace{\sum V\Delta R}_{F_i} \tag{13}$$

or, $G_i = A_{ij}\,F_i$.

where A represents the scattering coefficient matrix, F is the discrete frequency distribution of the particle size, and G is the actual attenuation coefficient measured for different frequencies.

Equation 13 is a classical ill-posed problem, therefore a regularization factor γ (the optimum factor i.e., a Lagrange multiplier used to find local minimum and maximum values) and a smoothing matrix H has been introduced by (Jia et al (2019)) to solve it as follows.

$$F = (A^T A + \gamma H) A^T G \quad \textbf{(14)}$$

In addition, an inversed Gaussian, can be employed to fit the particle size distribution (Lyon, (2014)). The general form of the inversed Gaussian distribution function is given by:

$$F(x) = \frac{1}{\sigma\sqrt{2\pi}} e^{-\frac{1}{2}\left(\frac{x - m_u}{\sigma}\right)^2} \quad \textbf{(15)}$$

where, m_u is the median of x variables and σ is the standard deviation.

The whole method described above is called *Optimum Regularization Technique ORT* (Su et al., (2007)). Figure 9 shows the measured particle size distribution of glass beads for the particle sizes considered (Table 1) by inversion of the measured attenuation coefficient.

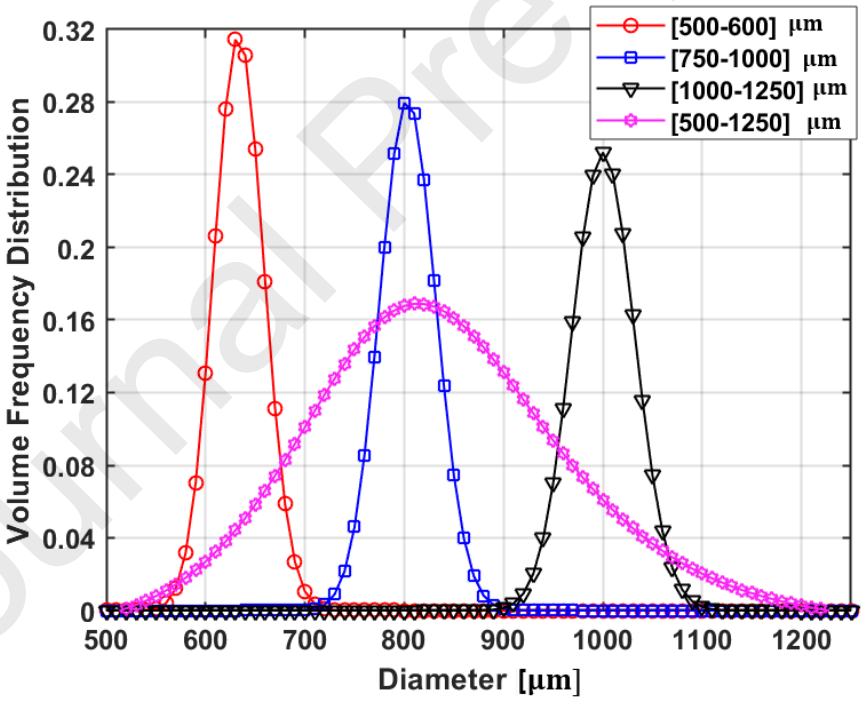

Figure 9: Inversed particle size distribution from the measured attenuation coefficient of glass beads with various particle sizes.

Figure 9 shows that the ultrasound technique can reliably measure online particle size distribution in highly concentrated particle suspensions. The particle size distributions of samples 1, 2, and 3 were also measured from image analysis (see Figure 2). The results

demonstrate that the widest PSD is found for sample 3. As can be seen in Figure 9, the ultrasound spectroscopy measurements gave a narrower size distribution compared to image analysis (see Figure 2), while the results from ultrasound are closer to the nominal particle sizes.

3.2a Segregation behaviour of particles in solid-liquid fluidized bed

In order to highlight the importance of the ultrasound attenuation technique as a diagnostic tool, the experimental setup 2 and the methodology described above were employed to investigate the segregation behaviour of the particles in sample 4 (see Table 1) at different fluidization conditions. The transducers were mounted at a height of 6.5 cm above the inlet distributor of the bed. The bed was initially run at a high superficial liquid velocity of ~ 6 cm/s for a while, to make sure that the particles were well mixed; after this the liquid flow was stopped abruptly. A visual check was performed to make sure that the particle sizes were actually mixed (Figure 10a). This check was possible thanks to the different colours of the ballotini particles of different sizes. The liquid superficial flow velocity was then increased again to specific values in between the minimum fluidization velocities of the different particle sizes. Specifically, the chosen velocities were $U/U_{mf} = 0$, $U/U_{mf} = 1.35$, and $U/U_{mf} = 4.37$, see Figure10.

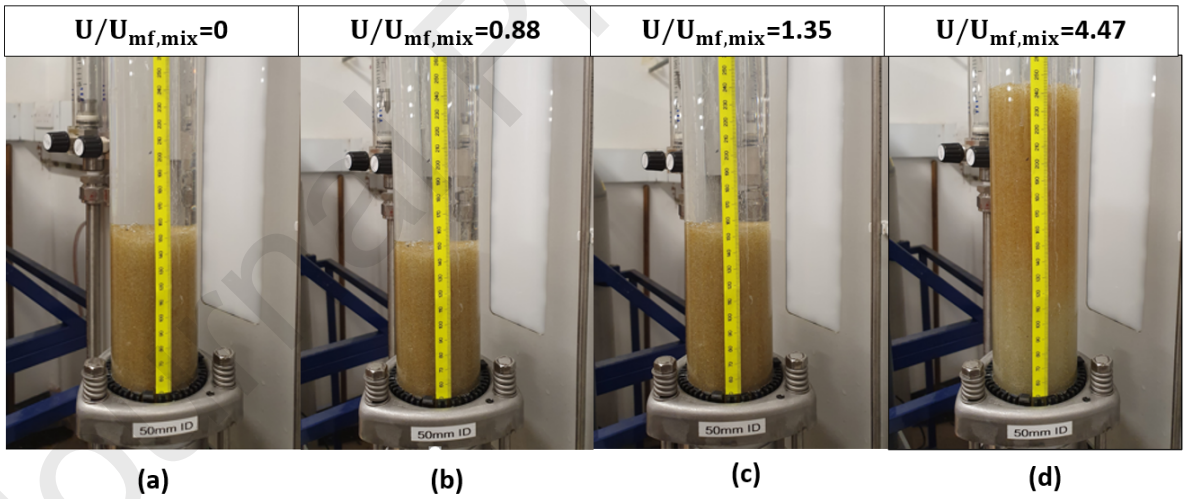

Figure 10: Image of the solid-liquid fluidized bed at various fluidization conditions.

Four different fluidization conditions are here considered and described:

- For superficial velocities significantly smaller than the mixture minimum fluidization velocity (Figure 10a) the bed is at rest and still well mixed since the particles have not started moving.

- As the water flow rate through the bed increases, the smallest particles are the first ones to start fluidizing, even for values of superficial velocity slightly smaller than the mixture minimum fluidization velocity, such as in Figure 10b. Here, $U/U_{mf,mix}=0.88$, meaning that the superficial velocity is lower than the mixture fluidization velocity. On the other hand, however, $U/U_{mf,sample\ 2}=1.13$, implying that the liquid superficial velocity is larger than the minimum fluidization velocity of the smaller particles (750-1000um). This leads to an incipient segregation, as the smallest particles migrate and end up near the top of the bed. However, some of these small particles remain stuck in between the large ones at the lower parts of the bed that have not fluidized yet.
- As the flowrate is further increased beyond the mixture minimum fluidization velocity (Figure 10c-d), all particles are fluidized and segregation is free to happen, causing the larger particles to drop to the bottom of the bed, while the smaller ones reach the top. This phenomenon is more evident for larger water flow rates (Figure 10d) since the drag force on each particle increases both with the superficial velocity and with the particle size. Therefore, the difference in between the forces acting on the particles of different sizes increases with the superficial velocities.
- If the flowrate is increased even more, turbulent mixing might prevail over this segregation phenomenon and, at least partially, restore the even distribution of particles of different sizes across the bed. This fluidization condition, however, was not achievable with the experimental setup used, as the upper limit on the water flow rate was too low to see a significant effect of turbulent mixing.

Since all the particles are made of the same material, and therefore have the same density, no layer inversion is expected to occur (Di Felice, (1995)). The corresponding measured attenuation coefficients of sample 4 are shown in Figure 11a, and the particle size distributions at 6.5 cm height, calculated from the inversion of the experimentally measured attenuation coefficients, are shown in Figure 11b.

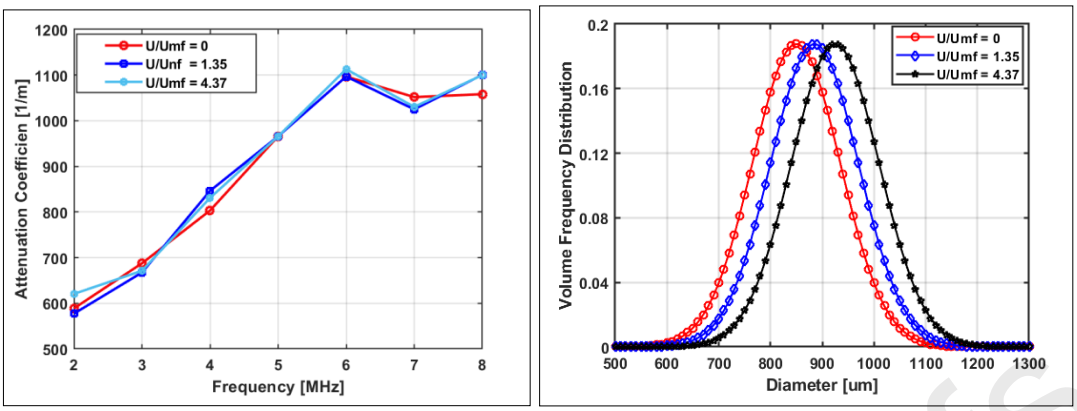

(a) (b)

Figure 11: (a) Ultrasonic attenuation coefficient spectra for glass bed particles sample 4 (see Table 1), (b) Inversed particle size distribution from the measured attenuation coefficient of glass beads for sample 4 (see Table 1)

The results of the ultrasound experiments seem to agree with the expectations: for fluid velocities below the minimum fluidization velocity of the smaller particles, no particles fluidized, and the particle size distribution at 6.5 cm above the distributor mesh returns an average value between the size ranges of sample 4. As the flow rate is increased above the mixture minimum fluidization velocity $U/U_{mf} = 1.35$, a shift of the particle size distribution towards larger sizes in the lower region of the fluidized bed can be seen in Figure 11b. This agrees with the visual observations (Figure 10c). As the flow rate further increased to $U/U_{mf} = 4.37$ a larger shift of the particle size distribution towards larger sizes can be seen in Figure 11b. The behaviour of the bed, for the range of velocities used, suggests that an increase in the fluidization velocity will cause an increase in the segregation, while mixing is expected to prevail only at flow rates larger than five times the mixture minimum fluidization velocity.

The results of PSD measurements are clearly indicating that the ultrasound technique has the potential to be used for the measurement of particles segregation in solid-liquid fluidized beds.

3.3 Particle Velocity Profile Measurements

For the measurement of the particle velocity profiles in the fluidized bed via the Doppler effect the experimental setup 3 is used. From the frequency shift of an acoustic wave between the sound source (Transducer T_1) and the particles that move relative to the ultrasound transducer, the Doppler effect can be used to determine the particle velocity distribution (Takeda. Y., (2013)). In this work, the ultrasound wave is propagated in the direction of the measurement

line, x (see Figure 1c) , at a depth x, with the maximum value for this depth, x_{max}, given by (Tomonori et al., (2013)):

$$x_{max} = \frac{C}{2f_{prf}} \tag{16}$$

where, C is the sound speed in the continuous phase (here is water), and f_{prf} is the pulse repetition frequency. The distance x of each reflected pulse towards the receiving transducer can be estimated from:

$$x = \frac{C}{2}t_i \tag{17}$$

where t_i is the reception time of each pulse. The signal is emitted by the transmitter transducer T_1 with frequency f_o. The transmitted signal is then scattered by the moving particles, and the scattered signal is received by the receiver transducer T_2 with frequency f_r . Owing to the motion of the particles relative to the transmitter transducer, the particles receive the transmitted signal with frequency f_1 found as:

$$f_1 = \frac{C + V\cos\theta}{C} f_o \tag{18}$$

where, V is the particles velocity, C is the sound speed in the continuous phase (water), and θ is the angle between the flow direction and the ultrasound beam axis. The frequency of the scattered wave f_r received by transducer T_2 is modulated by the motion of the particles relative to the transmitting transducer as:

$$f_r = \frac{C}{C - V\cos\theta} f_1 \tag{19}$$

Combining Equation 18 and Equation 19 we can find:

$$f_r = \left(1 + \frac{2V\cos\theta}{C - V\cos\theta}\right) f_o \tag{20}$$

The ultrasound velocity in fluid much larger than the particles velocity C>>V, then $C - V\cos\theta \approx C$, and Equation 20 becomes:

$$f_r = \left(1 + \frac{2V\cos\theta}{C}\right) f_o \tag{21}$$

The Doppler shift f_D can be expressed as:

$$f_D = f_r - f_o = \left(\frac{2V\cos\theta}{C}\right) f_o \tag{22}$$

From Equation 22 we understand that the frequency shift of the signal is proportional to the particle velocity (Tomonori et al., (2013)). The particle velocity V_i (where i is the number of reflected pulses) at each location along the measurement line x can be found by:

$$V_i(x) = \frac{C \quad f_{D_i,x}}{2\cos\theta \; f_o} \tag{23}$$

where, f_o is the frequency of the emitted signal, θ is the transducer inclination angle and $f_{D_i,x}$ is the frequency shift. To calculate the frequency shift, we used Fast Fourier Transform (FFT) on the received signal. The reflected pulses at each location i along the depth R_x will provide one peak frequency. The post-processing steps for the reconstruction of the velocity profiles are illustrated in Figure 12.

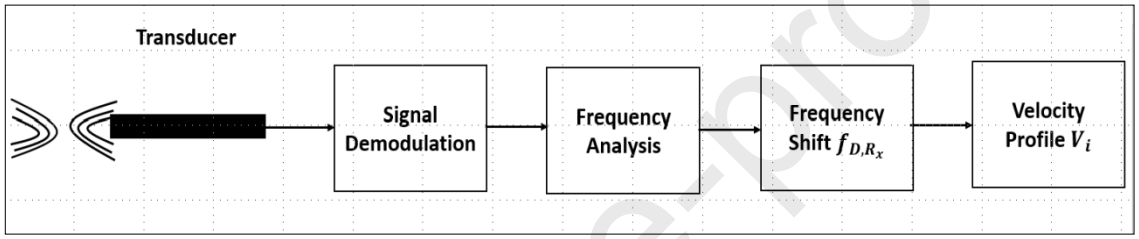

Figure 12: Signal processing for velocity profile measurements.

The signal is transmitted through the solid-liquid fluidized bed in burst mode with 4 sinusoidal cycles at a frequency of 5 MHz and sound speed C_s in the liquid-solid medium. The received signal $e(t)$ can be written as (Murakawa et al., (2014)):

$$e(t) = \sum_{i=0}^{N_{prf}-1} A_i \sin\left(2\pi f_o\left[t - t_i + f_{D_i,R_x}/f_{prf}\right]\right) + w[i] \tag{24}$$

where, t_i is the delay time (is calculated by measuring the reception time of each reflected pulse), A_i is the amplitude of the received signal, f_{prf} is the pulse repetition frequency and in our case is 100 Hz, N_{prf} is the number of pulse repetition frequency bins and $w[i]$ is the signal noise.

The received signal (echo signal) is demodulated by multiplying the samples by cosine and sine ($e^{-i(2\pi f_o t)}$) (Thong-un et al., (2018)), (see Equation 25), and low pass filtered.

$$Y(t) = \left[2e(t)e^{i(2\pi f_o t)}\right]_{\text{low Pass Filter}} = x_1(t) + ix_2(t) \tag{25}$$

where, $x_1(t)$ and $x_2(t)$ are the real and imaginary parts of $Y(t)$ respectively. If the signal is discrete then instead of $x_1(t)$ and $x_2(t)$ the discrete functions $X_1(i)$ and $X_2(i)$ are used,

The frequency shift can be estimated by:

$$f_{D_i,x} = \frac{1}{PRI}\frac{n(x)}{N} \quad \textbf{(26)}$$

where, PRI is the pulse repetition time interval between two adjusted pulses. The power spectrum density $n(x)$ was calculated from

$$n(x) = \frac{\sum_{i=0}^{N-1} i|C_{x,i}|^2}{\sum_{i=0}^{N-1}|C_{x,i}|^2} \quad \textbf{(27)}$$

where $C_{x,i}$ is the matrix element corresponding to the depth R_x and can be represented as FFT of ($X_1(i)$ and $X_2(i)$)

The Doppler shift frequency at depth x can be calculated by using Equation 26, and the velocity profiles are finally calculated by substituting $f_{D_i,x}$ into Equation 23 for all the depths along x. An example of the solid velocity profiles measured for particle sample 1 (see Table 3) is shown in Figure 13 at different liquid superficial velocities U. The measurement line x is not horizontal; a normalized x-axis is used where (x is divided by the bed diameter D).

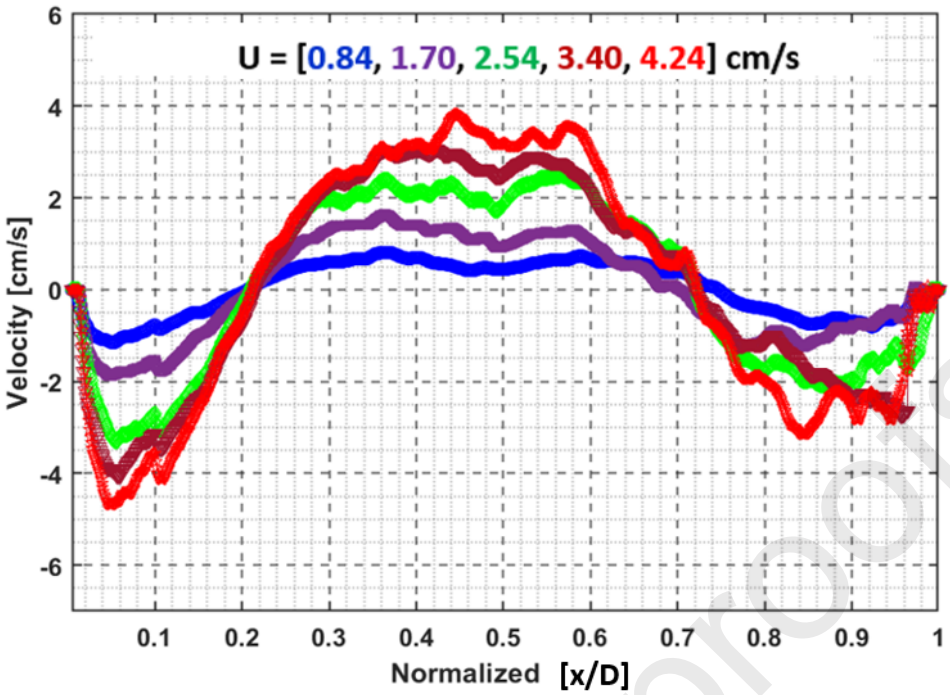

Figure 13: Velocity profiles measured in solid-liquid fluidized bed for sample 1 (see Table 1) at superficial liquid velocities U ranging from 0.8488 cm/s to 4.2441 cm/s (x is the depth, see Figure 1c, and D is the diameter of the fluidized bed).

The results show that the frequency shift increases as the liquid superficial velocity increases, since the particle velocities will also increase. From the velocity profile measurements in Figure 13, it appears that the particles inside the fluidized bed are circulating, having an upward motion in the centre of the bed and a downward one at the periphery. This agrees with findings from previous numerical studies (Limtrakul et al., (2005), Wang et al., (2010)).

4. Conclusions

Ultrasound techniques can potentially be a powerful tool for the determination of volume fraction, velocity profile, and particle size distribution of solid suspensions in liquids as encountered for example in fluidized bed systems. The system used for the experiments here consisted of a cylindrical fluidized bed with an inner diameter equal to 5 cm, a glass wall and a distributor mesh. The particles used were glass beads with diameter ranging between 500 and 1250 um and the fluidizing agent was water. Different ultrasound setups were used to obtain the different properties. For the measurement of the voidage, the attenuation coefficient and the transit time of the ultrasound wave through the solid-liquid mixture were used. The particle size

distribution was obtained by means of ultrasonic spectrometry. The ultrasonic attenuation coefficient was measured for a wide range of frequencies from 2-8 MHz. Combining the ultrasonic attenuation measurements and the *Optimum Regularisation Technique ORT* inversion algorithm, the size distributions of three different glass particle samples ranging from 500 μm to 1250 μm, were measured. The ultrasound technique was also used as a diagnostic tool to investigate the segregation behaviour of particles of different sizes at increasing fluidization velocities. Finally, the particle velocity profile in the fluidized bed was determined by the Doppler effect. The results showed that the particles moved upwards at the centre of the fluidized bed and downwards near the walls, indicating circulation patterns within the bed. These velocity profile shapes, and circulation patterns are in good agreement with literature results. The ultrasound measurement methods presented in this paper are not limited to solid-liquid fluidised beds but are applicable to any fluid-particle flows where the continuous phase is liquid.

Acknowledgments

The authors would like to acknowledge the support from Engineering and Physical Sciences Research Council, UK, through the PREMIERE Programme Grant (EP/T000414/1). M Errigo would like to acknowledge the Department of Chemical Engineering, UCL for the studentship.

5. References

ALLEGRA, J. R. & HAWLEY, S. A. (1972). Attenuation of sound in suspensions and emulsions: Theory and experiments. *J. Acoust. Soc. Am,* 51**,** 1545-1564.

ARITOMI, M., KIKURA, H. & SUZUKI, Y. (2000). Ultrasonic Doppler method for bubbly flow measurement. *Ohokayama, Meguro-Ku, Tokyo* 152**,** 1-20.

ATKINSON, C. M. & KYTO¨MAA, H. K. (1993). Acoustic Properties of Solid-Liquid Mixtures and the Limits of Ultrasound Diagnostics—I: Experiments (Data Bank Contribution). *Journal of Fluids Engineering,* 115**,** 665-675.

CHEN, J. L. P. & KEAIRNS, D. L. (1975). PARTICLE SEGREGATION IN A FLUIDIZED BED. *Canadian journal of chemical engineering,* 53**,** 1975.

CHUN, S., YOON, B. & LEE, K. B. (2011). Diagnostic flow metering using ultrasound tomography. *Journal of Mechanical Science and Technology,* 25**,** 1475-1482.

COCCO, R., KARRI, S. R. & KNOWLTON, T. (2014). Introduction to fluidization. *Chem. Eng. Prog,* 110**,** 21-29.

DI FELICE, R. (1995). Hydrodynamics of liquid fluidisation. *Chemical Engineering Science,* 50**,** 1213-1245.

DI RENZO, A., RITO, G. & DI MAIO, F. P. (2020). Systematic experimental investigation of segregation direction and layer inversion in binary liquid-fluidized bed. *Processes,* 8**,** 177.

DION, J. R. & BURNS, D. H. (2011). Determination of Volume Fractions in Multicomponent Mixtures Using Ultrasound Frequency Analysis. *Applied Spectroscopy,* 65**,** 648-656.

EVSEEV, A. R. (2016). Diagnostics of two-phase flows with high concentration of a solid dispersed phase using fiber-optic sensors.

GARBOWSKI, T., RICHTER, D. & PIETRYKA, M. (2019). Analysis of Changes of Particle Size Distribution and Biological Composition of Flocs in Wastewater During the Growth of Algae. *Water, Air, & Soil Pollution,* 230**,** 139.

GHATAGE, S. V., PENG, Z., SATHE, M. J., DOROODCHI, E., PADHIYAR, N., MOGHTADERI, B., JOSHI, J. B. & EVANS, G. M. (2014). Stability analysis in solid–liquid fluidized beds: Experimental and computational. *CHEM ENG J,* 256**,** 169-186.

HARKER, A. H. & TEMPLE, J. A. G. (1988). Velocity and attenuation of ultrasound in suspensions of particles in fluids. *Journal of Physics D: Applied Physics,* 21**,** 1576-1588.

HAY, A. E. & MERCER, D. G. (1985). On the theory of sound scattering and viscous absorption in aqueous suspensions at medium and short wavelengths. *The Journal of the Acoustical Society of America,* 78**,** 1761-1771.

HEAD, J. D. & ZERNER, M. C. (1985). A Broyden—Fletcher—Goldfarb—Shanno optimization procedure for molecular geometries. *Chemical Physics Letters,* 122**,** 264-270.

HOSSEIN, F. (2019). *Colloid Vibration Potential for Imaging in Engineering and Medicine.* University of Leeds.

HOSSEIN, F., MATERAZZI, M., LETTIERI, P. & ANGELI, P. (2021). Application of acoustic techniques to fluid-particle systems – A review. *Chemical Engineering Research and Design,* 176**,** 180-193.

HOSSEIN, F. & WANG, M. (2019). Colloid vibration potential imaging for medicine. *Journal of Biomedical Imaging and Bioengineering,* 3**,** 114-118.

HOSSEIN, F. & WANG, M. (2020). Modelling and measurement of ultrasound vibration potential distribution in an agar phantom. *Chemical Physics,* 534**,** 110757.

HUANG, Y. J., SUNG, C. C., LAI, J. S., LEE, F. Z., HWANG, G. W. & TAN, Y. C. (2013). Measurement of solid suspension concentration and flow velocity with temperature compensation using a portable ultrasonic device. *Hydrological Sciences Journal,* 58**,** 615-626.

IANNELLO, S., MORRIN, S. & MATERAZZI, M. (2020). Fluidised Bed Reactors for the Thermochemical Conversion of Biomass and Waste. *KONA Powder and Particle Journal,* 37**,** 114-131.

LAM CHEUN U, Y. V. (2010). Solids motion in fluidised beds of fine particles. ProQuest Dissertations Publishing.

LANGFORD, S., WIGGINS, C., TENPENNY, D. & RUGGLES, A. (2016). Positron Emission Particle Tracking (PEPT) for Fluid Flow Measurements. *Nuclear engineering and design,* 302**,** 81-89.

LAVERMAN, J. A., ROGHAIR, I., ANNALAND, M. V. S. & KUIPERS, H. (2008). Investigation into the hydrodynamics of gas-solid fluidized beds using particle image velocimetry coupled with digital image analysis. *CAN J CHEM ENG,* 86**,** 523-535.

LI, X.-L., CHEN, S.-J., LIU, S.-M. & LI, Z.-H. (2021)-a. AE waveform characteristics of rock mass under uniaxial loading based on Hilbert-Huang transform. *Journal of Central South University,* 28**,** 1843-1856.

LI, X., CHEN, S., WANG, E. & LI, Z. (2021)-b. Rockburst mechanism in coal rock with structural surface and the microseismic (MS) and electromagnetic radiation (EMR) response. *Engineering Failure Analysis,* 124**,** 105396.

LIMTRAKUL, S., CHEN, J., RAMACHANDRAN, P. A. & DUDUKOVIĆ, M. P. (2005). Solids motion and holdup profiles in liquid fluidized beds. *Chemical Engineering Science,* 60**,** 1889-1900.

LIN, C.-L., PENG, T.-H. & WANG, W.-J. (2011). Effect of particle size distribution on agglomeration/defluidization during fluidized bed combustion. *Powder Technology,* 207**,** 290-295.

LIU, J., GRACE, J. R. & BI, X. (2003). Novel multifunctional optical-fiber probe: II. High-density CFB measurements. *AICHE J,* 49**,** 1421-1432.

LYON, A. (2014). Why are normal distributions normal? *The British Journal for the Philosophy of Science,* 65**,** 621-649.

MACCHI, A., GRACE, J. R. & BI, H. T. (2001). Use of ultrasound for phase holdup measurements in multiphase systems. *Canadian Journal of Chemical Engineering,* 79**,** 570-578.

MATERAZZI, M., LETTIERI, P., DODDS, J. M. & MILLIKEN, A. (2017). X-ray imaging for design of gas nozzles in large scale fluidised bed reactors. *Powder Technology,* 316**,** 41-48.

MERIBOUT, M., SHEHZAD, F., KHAROUA, N. & KHEZZAR, L. (2020). An ultrasonic-based multiphase flow composition meter. *Measurement,* 161**,** 107806.

MORÉ, J. J. (1978). The Levenberg-Marquardt algorithm: implementation and theory. *Numerical analysis.* Springer.

MOSOROV, V. (2013). An iterative position reconstruction algorithm for radioactive particle techniques. *APPL RADIAT ISOTOPES,* 79**,** 56-61.

MUÑOZ-COBO, J. L., CHIVA, S., MÉNDEZ, S., MONRÓS, G., ESCRIVÁ, A. & CUADROS, A. J. L. (2017). Sensitivity of particle sizing by ultrasonic attenuation spectroscopy to material properties. . *Powder Technology,* 134**,** 243-248.

MURAKAWA, H., SUGIMOTO, K. & TAKENAKA, N. (2014). Effects of the number of pulse repetitions and noise on the velocity data from the ultrasonic pulsed Doppler method with different algorithms. *Flow Measurement and Instrumentation,* 40**,** 9-18.

NAN, J., MING-XU, S. & XIAO-SHU, C. (2019). Particle size distribution measurement based on ultrasonic attenuation spectra using burst superposed wave. *Results in Physic,* 13**,** 102273.

OBUSEH, C. C., FENG, Z.-G. & PAUDEL, B. D. (2012). An Experimental Study on Fluidization of Binary Mixture in Particulate Flows. *J DISPER SCI TECHNOL,* 33**,** 1379-1384.

OWOYEMI, O. (2007). CFD modelling of mono-component and binary gas-solid fluidized beds with application to industrial materials. ProQuest Dissertations Publishing.

PANARIELLO, L., MATERAZZI, M., SOLIMENE, R., SALATINO, P. & LETTIERI, P. (2017). X-ray imaging of horizontal jets in gas fluidised bed nozzles. *Chemical Engineering Science,* 164**,** 53-62.

PATRICIA, M. & DEREK, W. (2000). Characterization of particle size and its distribution during the crystallization of organic fine chemical products as measured in situ using ultrasonic attenuation spectroscopy. *Acoustical Society of America,* 109**,** 274-282.

SAADEVANDI, B. A. & TURTON, R. (2004). PARTICLE VELOCITY AND VOIDAGE PROFILES IN A DRAFT TUBE EQUIPPED SPOUTED-FLUIDIZED BED COATING DEVICE. *CHEM ENG COMMUN,* 191**,** 1379-1400.

SIGEL, B. (1998). A brief history of Doppler ultrasound in the diagnosis of peripheral vascular disease. *Ultrasound Med Biol,* 24**,** 169-76.

SINES, J. N., HWANG, S., MARASHDEH, Q. M., TONG, A., WANG, D., HE, P., STRAITON, B. J., ZUCCARELLI, C. E. & FAN, L.-S. (2019). Slurry bubble column measurements using advanced electrical capacitance volume tomography sensors. *Powder Technology,* 355**,** 474-480.

SPINELLI, E., MAURI, T., FOGAGNOLO, A., SCARAMUZZO, G., RUNDO, A., GRIECO, D. L., GRASSELLI, G., VOLTA, C. A. & SPADARO, S. (2019). Electrical impedance tomography in perioperative medicine: careful respiratory monitoring for tailored interventions. *BMC Anesthesiology,* 19**,** 140.

SU, M., XU, F., CAI, X., REN, K. & SHEN, J. (2007). Optimization of regularization parameter of inversion in particle sizing using light extinction method. *China particuology,* 5**,** 295-299.

SU, M., XUE, M., CAI, X., SHANG, Z. & XU, F. (2008). Particle size characterization by ultrasonic attenuation spectra. *Particuology,* 6**,** 276-281.

TAKEDA. Y. (2013). Instantanious velocity profile measurement by ultrasounic Doppler method. *JSME International Journal,* 38**,** 1995.

TAOFEEQ, H. & AL-DAHHAN, M. (2018). The impact of vertical internals array on the key hydrodynamic parameters in a gas-solid fluidized bed using an advance optical fiber probe. *Advanced Powder Technology,* 29**,** 2548-2567.

TEMKIN, S. (2000). Attenuation and dispersion of sound in dilute suspensions of spherical particles. *J ACOUST SOC AM,* 108**,** 126-146.

THAO, N., DAISUKE, S., TOMOHISA, N., HIDEYUKI, N. & QUI TRAN-CONG. M. (2016). Determination of particle size distribution and elastic properties of silica microcapsules by ultrasound spectroscopy. *Japanese Journal of Applied Physics* 55**,** 07KC01.

THONG-UN, N., WONGSAROJ, W., TREENUSON, W., CHANWUTITUM, J. & KIKURA, H. (2018). An experimental study of different signal processing methods on ultrasonic velocity profiles in a single phase flow. *Engineering Journal,* 22**,** 124-141.

TOMONORI, I., HIROSHIGE, K. & YASUSHI, T. (2013). Ultrasonic velocity profiler for very low velocity field. *Flow Measurement and Instrumentation's,* 34**,** 127-133.

TORTORA, P. R., CECCIO, S. L., MYCHKOVSKY, A. G., O'HERN, T. J. & TORCZYNSKI, J. R. (2008). Radial profiles of solids loading and flux in a gas–solid circulating fluidized bed. *Powder Technology,* 180**,** 312-320.

URIC, R. J. (1947). A Sound Velocity Method for Determining the Compressibility of Finely Divided Substances. *Journal of Applied Physics,* 18**,** 983-987.

VATANAKUL, M., ZHENG, Y. & COUTURIER, M. (2005). Ultrasonic Technique For Measuring Phase Holdups In Multiphase Systems. *Chemical Engineering Communications,* 192**,** 630-646.

WANG, S., LI, X., WU, Y., LI, X., DONG, Q. & YAO, C. (2010). Simulation of Flow Behavior of Particles in a Liquid−Solid Fluidized Bed. *Industrial & Engineering Chemistry Research,* 49**,** 10116-10124.

YANG, H., SU, M., WANG, X., GU, J. & CAI, X. (2016). Particle sizing with improved genetic algorithm by ultrasound attenuation spectroscopy. *Powder Technology,* 304**,** 20-26.

YANG, W. (2003). *Handbook of fluidization and fluid-particle systems / edited by Wen-Ching Yang,* New York, New York : Marcel Dekker.

YATES, J. G. & LETTIERI, P. (2016). *Fluidized-Bed Reactors: Processes and Operating Conditions.*, Cham : Springer International Publishing : Imprint: Springer.

Fria Hossein: Writing original draft, review and editing, data curation, formal analysis, experiments and methodology.

Matteo Errigo: Experiments, partial writing, editing.

Maximiliano Matterazzi: Review, editing.

Paola Lettieri: Supervision, review.

Panagiota Angeli: Supervision, editing, review, validation.

Highlights:

- This paper describes an application of ultrasound techniques to solid-liquid fluidized beds.
- The ultrasonic methods are used for obtaining velocity profiles, particle size distribution, and solids volume fraction.
- The solid velocity profiles and particle size distributions were measured for four different sizes of glass particles ranging from 500 μm to 1250 μm at a solid volume fraction of 35%.
- The importance of the techniques as a diagnostic tool to investigate the particles segregation behaviour in solid-liquid fluidized beds at different fluidization conditions are reported.

Declaration of interests

☐ The authors declare that they have no known competing financial interests or personal relationships that could have appeared to influence the work reported in this paper.

☒ The authors declare the following financial interests/personal relationships which may be considered as potential competing interests:

Fria Hossein reports financial support was provided by University College London. Corresponding Author and co-authors are employed by University College London